Basic Res Cardiol (2014) 109:411
DOI 10.1007/s00395-014-0411-3

ORIGINAL CONTRIBUTION

The adapter protein c-Cbl-associated protein (CAP) protects from acute CVB3-mediated myocarditis through stabilization of type I interferon production and reduced cytotoxicity

Alan Valaperti · Mototsugu Nishii · Youan Liu · Howard Yang · Kotaro Naito · Peter P. Liu · Urs Eriksson

Received: 20 June 2013 / Revised: 2 April 2014 / Accepted: 14 April 2014 / Published online: 24 April 2014

Abstract c-Cbl-associated protein (CAP), also called Sorbs1 or ponsin, has been described as an essential adapter protein in the insulin-signalling pathway. Here, we describe for the first time a unique protective role for CAP in viral myocarditis. Mortality and heart failure development were increased in $CAP^{-/-}$ mice compared to $CAP^{+/+}$ littermates after Coxsackievirus (CVB3) infection. Mechanistically, CAP protected from tissue apoptosis because of reduced $CD8^+$ T and natural killer cell cytotoxicity. Despite reduced cytotoxic elimination of CVB3-infected cells in $CAP^{+/+}$ hearts, however, CAP enhanced interferon regulatory factor 3 (IRF3)-dependent antiviral type I interferon production and decreased viral proliferation in vitro by binding to the cytoplasmic RIG-I-like receptor melanoma differentiation-associated protein 5 (MDA5). Taken together, these findings reveal a novel modulatory role for CAP in the heart as a key protein stabilizing antiviral type I interferon production, while protecting from excessive cytotoxic responses. Our study will help to define future strategies to develop treatments to limit detrimental responses during viral heart inflammation.

Keywords Myocarditis · Heart failure · Inflammation · Type I interferons · Perforin · Coxsackievirus

Introduction

c-Cbl-associated protein (CAP), also identified as Sorbs1 (Sorbin and SH3 domain-containing protein 1) or ponsin, belongs to the SoHo vinexin family of adapter proteins. Together with nectin and afadin, CAP composes the cell–cell adhesion system named NAP [22]. CAP interacts with several molecules, which modulate cell adhesion, cell migration, cytoskeleton, membrane trafficking, and intracellular signalling [17, 19, 47]. Remarkably, CAP has been described to be an essential adapter protein in the insulin-

P. P. Liu and U. Eriksson shared last authorship.

Electronic supplementary material The online version of this article (doi:10.1007/s00395-014-0411-3) contains supplementary material, which is available to authorized users.

A. Valaperti · M. Nishii · Y. Liu · H. Yang · K. Naito · P. P. Liu
Division of Cardiology, Heart and Stroke/Richard Lewar Centre of Excellence, Toronto General Hospital Research Institute, University Health Network, University of Toronto, Toronto, Ontario, Canada

A. Valaperti (✉) · U. Eriksson
Division of Cardioimmunology, Center for Molecular Cardiology, University of Zurich, Schlieren, Switzerland
e-mail: alan.valaperti@vetbio.uzh.ch

A. Valaperti
Institute of Veterinary Biochemistry and Molecular Biology, University of Zurich, Zurich, Switzerland

M. Nishii
Department of Angio-Cardiology, Kitasato University School of Medicine, Kanagawa, Japan

P. P. Liu
University of Ottawa Heart Institute, University of Ottawa, Ottawa, Ontario, Canada

U. Eriksson
Department of Medicine, GZO-Zurich Regional Health Center, Wetzikon, Switzerland

signalling pathway forming a complex with Cbl and flotillin, the latter being localized to the lipid raft of the cellular plasma membrane [5]. Structurally, CAP is localized with actin cytoskeleton, stress fibres, focal adhesion, cell–cell adhesion structures, and has been also found in the cellular nucleus [18, 29, 46].

c-Cbl-associated protein is mainly expressed in heart, skeletal muscle, adipose tissue, and macrophages [19, 30]. Studies on a mouse model of high-fat diet-induced insulin resistance recently suggested a pro-inflammatory role for CAP. Accordingly, high-fat diet feeding increased pro-inflammatory cytokine and chemokine release from macrophages [19]. Despite the fact that a role of CAP in viral infection has not been described yet, these observations point toward a potential regulatory role of CAP in the innate immune system.

Together with Toll-like receptors TLR3, TLR4, TLR7, and TLR9, the PPR retinoic acid-induced gene I (RIG-I)-like receptors (RLRs) melanoma differentiation-associated protein 5 (MDA5) and RIG-I, identify virus particles and, in addition to NF-κB nuclear translocation, induce TBK1/IKKε-dependent activation of interferon regulatory factors (IRFs) which results in the production of antiviral interferons (IFNs) [2, 16]. In particular, IRF3 plays a critical role in IFN-β production, while IRF7 regulates both IFN-α and IFN-β [15, 32].

The Coxsackie virus B3 (CVB3), a cardiotropic positive single-strand RNA (+ssRNA) enterovirus, is an important cause of myocarditis, which often progresses to end-stage heart failure [31]. TLR3 and MDA5 recognize CVB3 double-strand RNA in the intracellular endolysosome or directly in the cytosol, respectively [2, 16, 44]. Another RLR helicase, RIG-I, recognizes negative single-strand RNA (-ssRNA) viruses such as the vesicular stomatitis virus (VSV) [16]. After infection, TLR3/MDA5- or TLR3/RIG-I-triggered type I IFNs on one side, and cytotoxic $CD8^+$ T cells and NK cells eliminating virus-infected cells on the other side, limit virus expansion in the host [3, 11]. In the presence of severe infection, however, perforin-induced cytolysis may trigger extensive pro-apoptotic signalling pathways in heart tissue [3]. Extensive tissue damage together with a strong systemic inflammatory response, on the other hand, predisposes to heart-specific autoimmunity and heart failure progression [9].

c-Cbl-associated protein has several functions and is highly expressed in the heart. Since a role for CAP in antiviral protection has not yet been elucidated, we aimed to clarify whether CAP may influence antiviral responses in cardiac diseases. To this end, we used a mouse model of Coxsackievirus-induced myocarditis to demonstrate the novel and beneficial dual role of CAP.

Results

CAP protects from CVB3-induced myocarditis

To clarify the in vivo role of CAP in viral heart disease, we infected $CAP^{-/-}$ mice and $CAP^{+/+}$ littermate controls with CVB3 and analysed mortality, cardiac function, and myocarditis severity. In $CAP^{+/+}$ mice, CAP was constitutively expressed at the RNA level before infection, decreased until day 4 after infection, and raised again until day 7 post infection (p.i.) (Fig. 1a). Survival curve showed enhanced mortality in $CAP^{-/-}$ mice compared to $CAP^{+/+}$ littermate controls in the first week of infection during acute myocarditis (Fig. 1b). Cross sections of H&E-stained infected hearts showed higher disease scores in $CAP^{-/-}$ compared to $CAP^{+/+}$ hearts at day 7 (Fig. 1c, left and right). Echocardiography demonstrated impaired fractional shortening in CVB3-infected $CAP^{-/-}$ mice compared to $CAP^{+/+}$ controls at day 7 (Fig. 1d, Suppl. Fig. S1).

Despite the fact that overall disease scores did not differ at day 4, flow cytometry showed higher percentages of heart-infiltrating dendritic cells and macrophages in infected $CAP^{+/+}$ hearts at this time point (Fig. 1e, Suppl. Fig. S1b). In contrast, cytotoxic NK and $CD8^+$ T cells among $CD45^{high}$- and $CD3^+$-expressing cardiac infiltrates, respectively, were higher in $CAP^{-/-}$ mice compared to $CAP^{+/+}$ mice (Fig. 1e, f, Suppl. Fig. S1b, c). $CD4^+$ T cells, however, showed higher percentages in infected $CAP^{+/+}$ hearts compared to $CAP^{-/-}$ hearts (Fig. 1f, Suppl. Fig. S1c).

Taken together, these observations suggest that CAP exerts a protective effect in CVB3-mediated viral myocarditis. Compared to $CAP^{-/-}$ hearts, $CAP^{+/+}$ hearts show enhanced infiltrations with cells of myeloid origin, such as dendritic cells and macrophages, but reduced cytotoxic cells of lymphoid origin, such as $CD8^+$ T cells and NK cells.

Enhanced lymphocyte activation in the absence of CAP

Levels of $CD3^+$ T cells, cytotoxic $CD8^+$ T cells, and $CD49b^+CD3^-$ NK cells showed only non-significant differences in spleens of non-infected $CAP^{+/+}$ vs. $CAP^{-/-}$ mice at baseline (Suppl. Fig. S2a, b). After CVB3 infection, however, percentages of $CD8^+CD44^{high}$ T cells and $CD49b^+CD3^-$ NK cells became significantly higher in spleens of $CAP^{-/-}$ mice compared to $CAP^{+/+}$ controls (Fig. 2a, b, Suppl. Fig. S2c). In contrast, percentages of effector $CD4^+CD44^{high}$ T cells remained almost comparable in both $CAP^{+/+}$ and $CAP^{-/-}$ spleens (Fig. 2a, Suppl. Fig. S2c). Similarly, we found more heart-infiltrating cytotoxic CD8 T and NK cells in $CAP^{-/-}$ compared to $CAP^{+/+}$ mice after CVB3 infection (Fig. 1e, f).

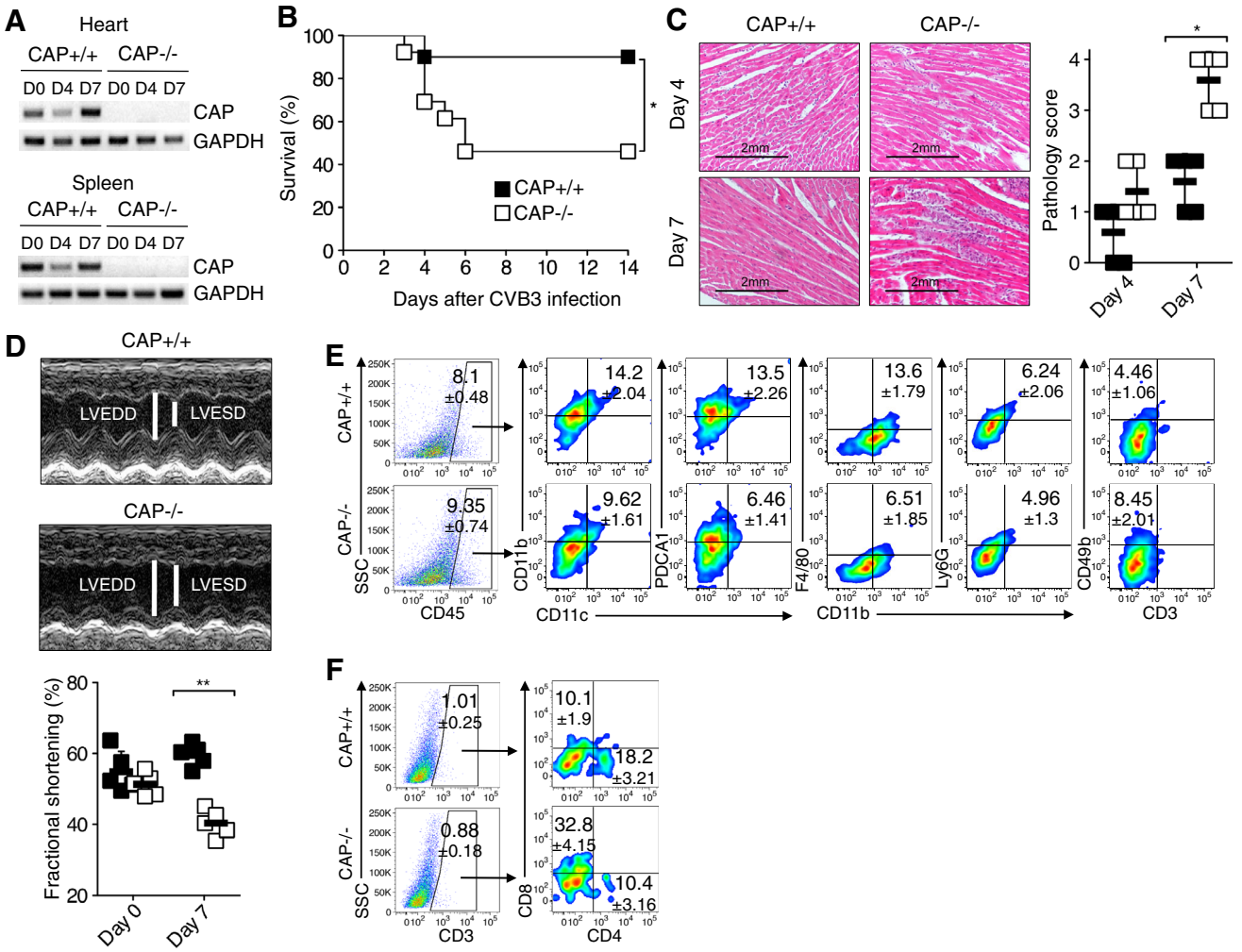

Fig. 1 CAP protects from CVB3-induced myocarditis. **a** Quantitative RT-PCR analysis of CAP RNA expression in hearts and spleens before, 4, and 7 days after CVB3 challenge. **b** Survival rates of age- and sex-matched $CAP^{+/+}$ ($n = 20$) and $CAP^{-/-}$ ($n = 20$) mice injected with $5 \times 10e4$ pfu/mouse CVB3. Log-rank test, $*P = 0.0368$. **c** *Left*—hematoxylin and eosin staining of $CAP^{+/+}$ and $CAP^{-/-}$ heart cross sections. *Right*—pathological scores evaluating heart-infiltrating cells from score 0 to score 4 according to the range previously described [25]. Magnification ×200. **d** Cardiac function of mice at the baseline before CVB3 infection and 7 days after CVB3 infection was assessed by echocardiography ($n = 7$ each group). Left ventricular diameters were determined by transthoracic M-mode echocardiographic tracings. LV fractional shortening (FS) was calculated using the formula FS = [(LVEDD − LVESD)/LVEDD] × 100. **e** Flow cytometry analysis of heart-infiltrating cells of the innate immune system 4 days post infection. Triple staining of $CD45^{high}$-gated heart-infiltrating $CD11c^{+}CD11b^{+}$ myeloid DC, $CD11c^{+}PDCA1^{+}$ plasmacytoid DC, $CD11b^{+}F480^{+}$ monocytes/macrophages, $CD11b^{+}Ly6G^{+}$ granulocytes, $CD49b^{+}CD3^{-}$ natural killer (NK) cells. At least 200,000 events have been acquired from a live gate. **f** Flow cytometry analysis of heart-infiltrating T cells 4 days post infection. Triple staining of $CD3^{+}$-gated heart-infiltrating $CD4^{+}$ and $CD8^{+}$ T cells. At least 200,000 events have been acquired from a live gate. Data are representative for two independent experiments (**a**, **c**, **e**, **f**), $n = 5$ each group if not otherwise described (mean, SD). $*P < 0.05$, $*P < 0.01$ (Student's t test)

Lymphocytes activation and proliferation critically involve T cell receptor (TCR) downstream molecules such as the cytoplasmic signal transducer Lck and Zap-70 [38]. Phosphorylation of the Src family protein tyrosine kinase Lck at the regulatory tyrosine Y192, which in turn induces Zap-70 phosphorylation and amplifies TCR signal transduction and cytokines production [48], was increased in $CAP^{-/-}$ splenocytes (Fig. 2c).

Beside antiviral cytokines, Lck and the transmembrane receptor CAR directly determine CVB3 infectivity [21]. We therefore measured CAR and Lck in CVB3-infected hearts, and found that their expression was CAP independent (Suppl. Fig. S2d). To better characterise T cell activation level, we measured the activation marker CD69. Consistently, we observed higher CD69 expression in $CAP^{-/-}$ than in $CAP^{+/+}$ T cells after in vitro stimulation (Fig. 2e).

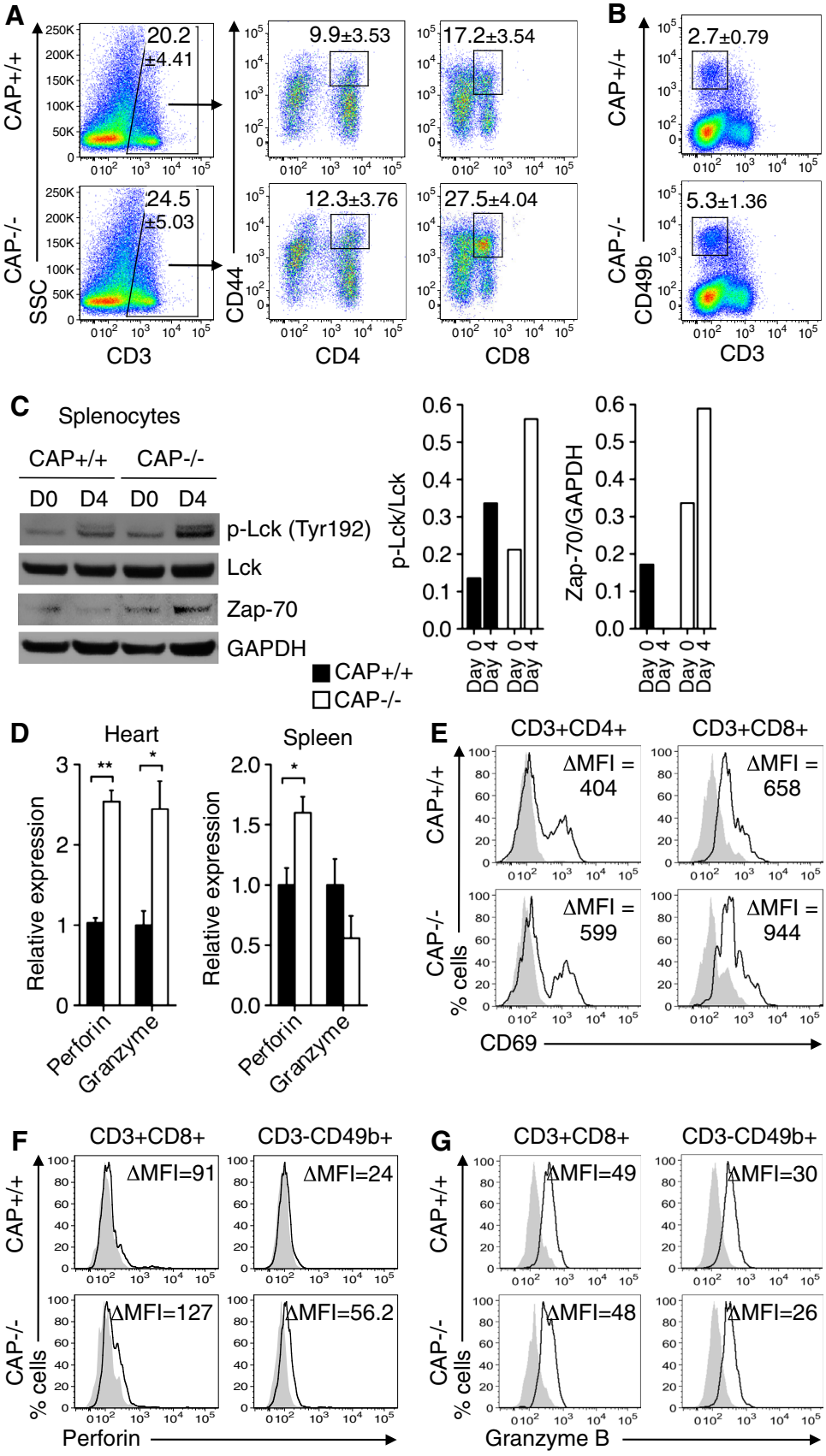

Fig. 2 Limited activation of cytotoxic lymphocytes in the presence of CAP. **a**, **b** Flow cytometry analysis of $CD3^+CD4^+CD44^{high}$ and $CD3^+CD8^+CD44^{high}$ effector T cells (**a**) and $CD3^-CD49^+$ NK cells (**b**) in the spleen of infected mice 4 days after CVB3 challenge. **c** (*Left*) Immunoblot analysis of p-Lck, total Lck, total Zap-70, and GAPDH in lysed splenocytes suspensions before and 4 days after CVB3 infection. (*Right*) Ratio between the densitometric evaluation of p-Lck and total Lck, and the densitometric evaluation of Zap-70 and GAPDH. **d** Quantitative RT-PCR analysis of cytolytic perforin and granzyme B 4 days after CVB3 infection in hearts and spleens. **e** Expression of the activation marker CD69 on splenocytes suspensions simulated in vitro with plate-bound CD3/CD28 antibodies for 48 h. Analysis was performed by flow cytometry. **f, g** Intracellular flow cytometry analysis of splenocytes suspensions stimulated in vitro with plate-bound CD3/CD28 antibodies for 48 h. Perforin (**f**) and granzyme B (**g**) production was detected in cytotoxic $CD3^+CD8^+$ T cells and $CD3^-CD49b^+$ NK cells. Data are representative for two independent experiments (**e**–**g**), $n = 5$ each group (**a**–**d**) (mean, SD). $^*P < 0.05$, $^*P < 0.01$ (Student's t test)

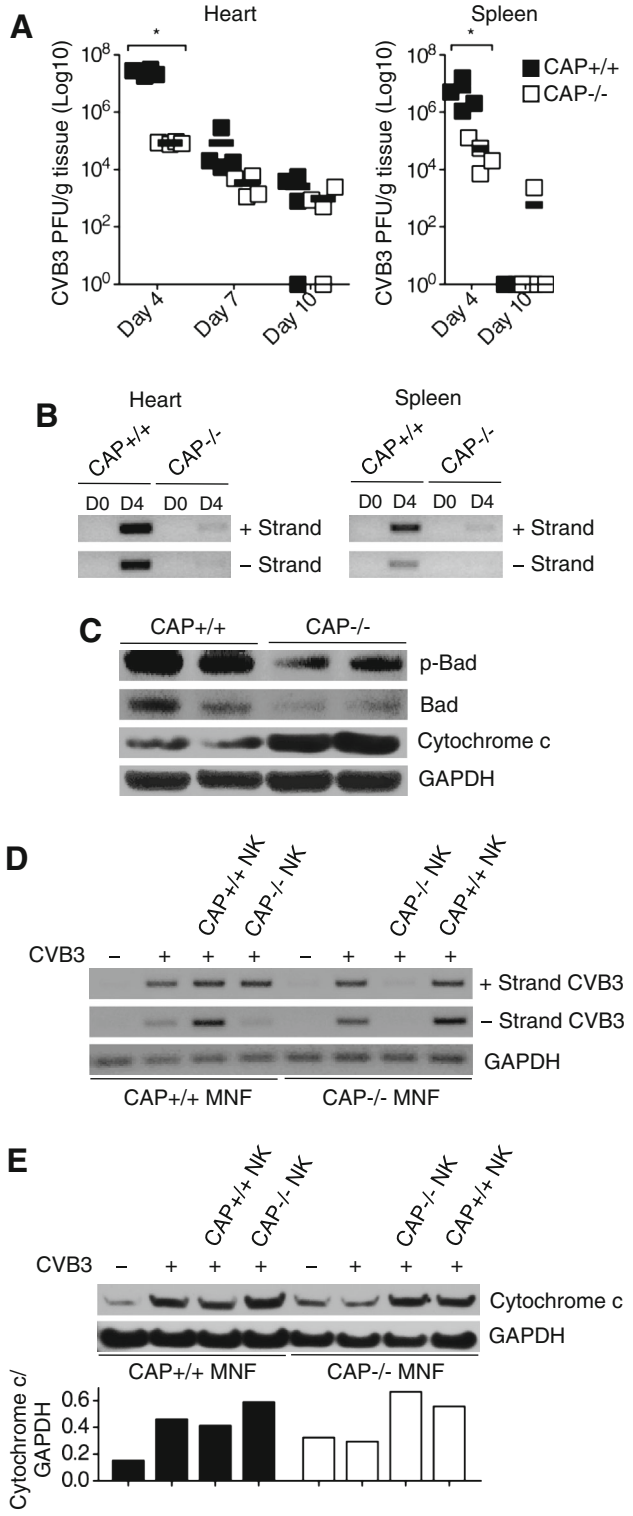

◀**Fig. 3** CAP limits pro-apoptotic cytotoxic responses. **a** Plaque-forming assay of heart and spleen lysates collected 4, 7, and 10 days after CVB3 infection. **b** Semi-quantitative RT-PCR analysis of CVB3 (+)-strand RNA infection and CVB3 (−)-strand RNA replication in $CAP^{+/+}$ and $CAP^{-/-}$ hearts and spleens before and 4 days after CVB3 infection. **c** Immunoblot analysis of p-Bad, total Bad, Cytochrome c, and GAPDH in heart tissue lysates 4 days after CVB3 infection. **d** Semi-quantitative RT-PCR analysis of CVB3 (+)-strand RNA infection and CVB3 (−)-strand RNA replication in $CAP^{+/+}$ and $CAP^{-/-}$ mouse neonatal cardiac fibroblasts (MNF) (2×10^5 cells) co-cultivated with $CAP^{+/+}$ or $CAP^{-/-}$ NK cells (2×10^5 cells), E:T ratio 1:1, infected with 1 MOI CVB3 (+) or left uninfected (−) for 24 h. GAPDH was used as internal loading control. **e** Immunoblot analysis of Cytochrome c in MNF after co-cultivation with NK cells, infected with 1 MOI CVB3 (+) or left uninfected (−) for 24 h, as described in (**d**). Data are representative for two independent experiments (**a**–**c**), $n = 5$ each group, or three independent experiments (**e**, **f**) (mean, SD). $^*P < 0.05$ (Student's t test)

Interestingly, we measured comparable expression of co-stimulatory molecules CD40, CD80, and CD86, as well as MHCII, on antigen presenting $CAP^{+/+}$ and $CAP^{-/-}$ cells after in vitro stimulation (Suppl. Fig. S3a, b).

Efficient CVB3 clearance despite reduced CD8 T and NK cell responses in $CAP^{+/+}$ compared to $CAP^{-/-}$ mice

$CD8^+$ T cell- and NK cell-induced cytotoxicity is largely mediated by perforin, which lyse virus-infected cells and eliminate the offending virus [11]. CAP inhibited expression and production of perforin in hearts and spleens after CVB3 infection and after in vitro stimulation (Fig. 2d, f). Like perforin, granzyme B was similarly increased in hearts of CVB3-infected $CAP^{-/-}$ mice (Fig. 2d). Its expression in CVB3-infected spleens and in vitro-stimulated splenic cells, however, showed comparable levels between $CAP^{+/+}$ and $CAP^{-/-}$ (Fig. 2d, g). In line with increased cardiac infiltrations of CD8 T and NK cells in CVB3-infected $CAP^{-/-}$ mice, both virus titers and viral proliferation were reduced in hearts and spleens of $CAP^{-/-}$ mice 4 days after infection (Fig. 3a, b). At day 10, however, plaque assays showed comparably low virus titers in hearts and spleens of both $CAP^{-/-}$ and $CAP^{+/+}$ mice (Fig. 3a).

Checking the typical cytokine expression patterns of activated primary T and NK cells in vitro, we observed that IL-17A, but not IFN-γ, was higher in $CAP^{-/-}$ than in $CAP^{+/+}$ splenic $CD4^+$ T cells, cytotoxic $CD8^+$ T, and NK cells (Suppl. Fig. S4a). Beside its role in $CD4^+$ Th1 lineage commitment, the transcription factor T-bet, as well as the transcription factor Eomes, also critically regulates the cytolytic effector mechanism of $CD8^+$ T cells and NK cells [40]. In fact, we found significantly increased expression of T-bet and Eomes in spleens of $CAP^{-/-}$ mice 4 days after infection (Suppl. Fig. S4b, c). In addition, and in accordance with higher IL-17A production in $CAP^{-/-}$ cells, the Th17 transcription factor RORγ was highly expressed in $CAP^{-/-}$ mice (Suppl. Fig. S4b).

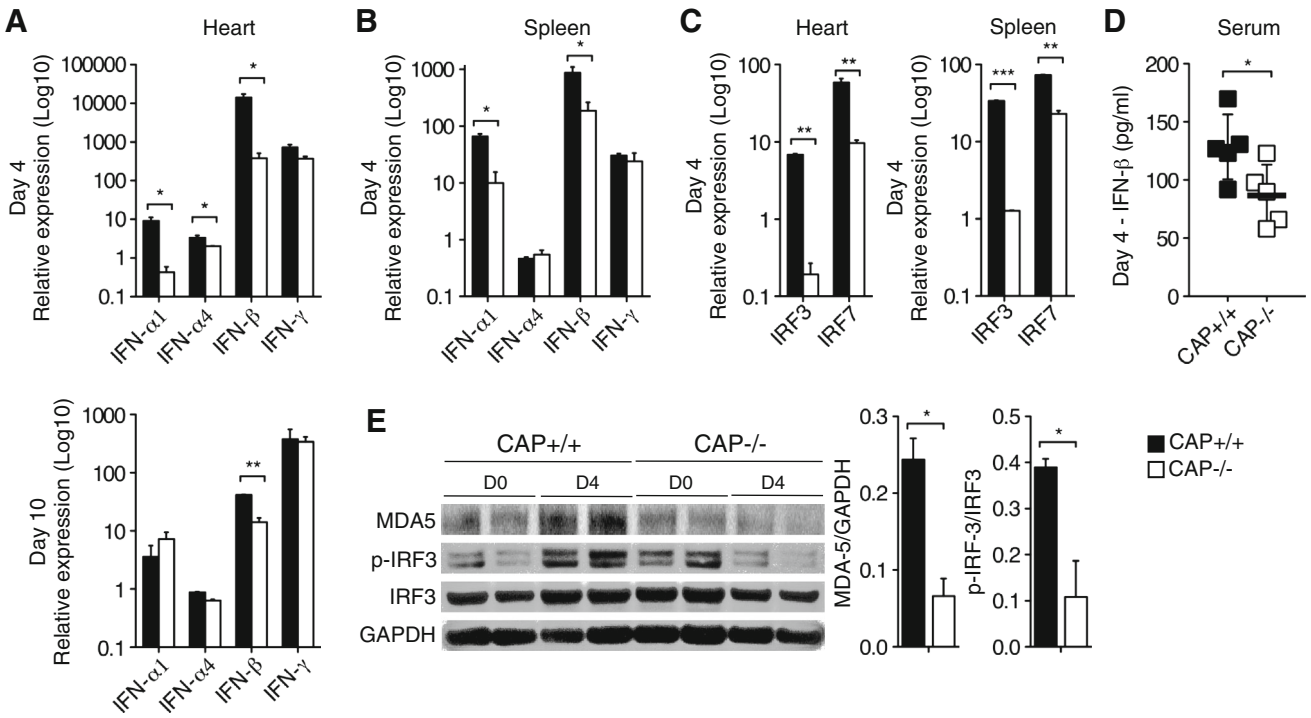

Fig. 4 CAP promotes type I IFNs production in vivo. **a**, **b** Quantitative RT-PCR analysis of RNA expression of antiviral type I (IFN-α1, IFN-α4, and IFN-β) and type II (IFN-γ) IFNs in the heart 4 and 10 days after CVB3 infection (**a**) and in the spleen at day 4 post CVB3 infection (**b**). **c** Quantitative RT-PCR analysis of RNA expression of the two major type I IFNs transcription regulators, namely IRF3 and IRF7, in hearts and spleens 4 days post CVB3 infection. **d** Concentration of IFN-β proteins measured by ELISA in blood serum collected from mice 4 days after CVB3 infection. **e** Immunoblotting analysis of MDA5, p-IRF3, and IRF3 in heart lysates before and 4 days after CVB3 infection. Densitometry values normalized to GAPDH are shown on the right. Data are representative for two independent experiments, $n = 5$ each group (mean, SD). $^{*}P < 0.05$, $^{**}P < 0.01$, $^{***}P < 0.001$ (Student's t test)

CAP protects from virus-induced apoptosis

In view of the markedly enhanced mortality and impaired cardiac function in $CAP^{-/-}$ mice compared to $CAP^{+/+}$ mice, we hypothesized that the increased cytotoxic response in the absence of CAP might promote activation of pro-apoptotic pathways in $CAP^{-/-}$ mice. To prove this hypothesis, we measured major pro-apoptotic molecules Bad and Cytochrome c in CVB3-infected hearts. Bad is inactive in its phosphorylated form, but when de-phosphorylated, contributes to Cytochrome c release from the mitochondria activating several caspases, which ultimately mediate apoptosis [8]. As expected, $CAP^{-/-}$ hearts showed lower levels of inactive, phosphorylated Bad (Fig. 3c). Consistently, $CAP^{-/-}$ hearts expressed higher amounts of Cytochrome c compared to $CAP^{+/+}$ hearts (Fig. 3c). To test if enhanced apoptotic signals in $CAP^{-/-}$ mice were directly mediated through cytotoxic cells, we co-cultivated mouse neonatal cardiac fibroblasts (MNF) and NK cells in vitro. As observed in Fig. 3d and e, $CAP^{-/-}$ NK cells strongly inhibited viral proliferation on one side, but also promoted high levels of pro-apoptotic Cytochrome c release on the other side. It is know that the activation of the PI3K/Akt pathway modulates apoptosis. However, we excluded that the PI3K/Akt pathway determined apoptosis in the absence of CAP, since CVB3-infected mice did not show any difference between $CAP^{+/+}$ and $CAP^{-/-}$ in phosphorylated PI3K and Akt in spleens and hearts (Suppl. Fig. S5a, b).

CAP promotes type I IFNs production in vivo

So far, we provided evidence that CAP protects from virus-triggered tissue damage and cytotoxicity in CVB3-mediated myocarditis. Efficient clearance of infective agents, however, had proven critical for host survival in the long term. We therefore asked how the CVB3-infected organism controls viral load while reducing the cytotoxic effect of CD8 T and NK cells. Given the importance of interferons during early antiviral defence, we therefore addressed whether and how CAP regulates type I and II IFNs. Accordingly, we measured RNA expression levels of type I and II IFNs, IRF3, and IRF7 in $CAP^{+/+}$ and $CAP^{-/-}$ after CVB3 infection. RNA expression of all type I IFNs tested,

namely IFN-α1, IFN-α4, and IFN-β, was higher in $CAP^{+/+}$ hearts at day 4 p.i, and partially at day 10 p.i. compared to $CAP^{-/-}$ hearts, while IFN-γ did not differ (Fig. 4a). Similarly, IFN-α1 and IFN-β, but not IFN-α4 and IFN-γ, were expressed at higher levels in $CAP^{+/+}$ spleens compared to $CAP^{-/-}$ spleens at day 4 p.i. (Fig. 4b). Enhanced RNA levels of the major type I IFNs transcription factors IRF3 and IRF7 in $CAP^{+/+}$ hearts and spleens at day 4 post-CVB3 infection confirmed these results (Fig. 4c). To test if CAP may influence type I IFN-dependent antiviral protection at the protein level, we collected blood serum from CVB3-infected mice at day 4. Consistent with the RNA expression data, analysis by ELISA showed that $CAP^{+/+}$ mice produced higher levels of IFN-β than $CAP^{-/-}$ mice (Fig. 4d). In addition, phosphorylation of IRF3, which indicates IRF3 nuclear translocation and promotion of type I IFNs transcription, was increased in $CAP^{+/+}$ hearts at day 4 post infection, while $CAP^{-/-}$ hearts showed only minimal IRF3 phosphorylation (Fig. 4e).

MDA5, a cytosolic receptor recognizing CVB3 double-strained RNA and triggering IRF3 phosphorylation [43], is usually cleaved and degraded by CVB3 to limit type I IFN-dependent host defence [4, 42]. We observed that CAP prevented MDA5 from degradation at the protein level in the heart after CVB3 infection (Fig. 4e).

Taken together, CAP promotes type I IFN-dependent antiviral protection in acute CVB3-induced myocarditis.

CAP supports type I IFN-dependent antiviral protection in vitro

To test how CAP promotes type I IFNs production in vitro, we next stimulated MEF, BMDC, and BMM with ligands for TLR3 (PolyIC), TLR7 (R848), MDA5, and RIG-I and measured IFN-β and IFN-α1 induction. Since MDA5 and RIG-I are cytosolic RLRs helicases, we induced activation of MDA5 and RIG-I by transfecting cells with HMW-PolyIC and LMW-PolyIC, respectively [27]. ELISA was used to analyse IFN-β at the protein level in supernatants, while IFN-β and IFN-α1 RNA levels were measured by qRT-PCR. We found that TRL3 and TLR7 ligands, as well as RIG-I, induced comparable amounts of IFN-β in both $CAP^{+/+}$ and $CAP^{-/-}$ cells (Fig. 5a), while MDA5 ligand induced higher levels of IFN-β in $CAP^{+/+}$ cells than in their $CAP^{-/-}$ counterparts (Fig. 5b, c). Similar to stimulation with HMW-PolyIC, which mimics viral (+)RNA ligands for MDA5, infection with CVB3 led to significantly higher levels of IFN-β in $CAP^{+/+}$ BMDM compared to $CAP^{-/-}$ BMDC, while VSV infection, similar to LMW-PolyIC, which mimics viral (-)RNA ligands for RIG-I, showed comparable IFN-β production in both cells (Fig. 5d, e). IFN-α1 levels were differently over-expressed in $CAP^{+/+}$ and $CAP^{-/-}$ cells. Upon HMW-PolyIC stimulation, IFN-α1 and IFN-β RNA levels were higher in $CAP^{+/+}$ BMDC. $CAP^{+/+}$ and $CAP^{-/-}$ MEF, however, showed comparable IFN-α1 expression (Fig. 5c, d). Similarly, comparable IFN-α1 over-expression was observed in $CAP^{+/+}$ and $CAP^{-/-}$ BMDC and MEF after CVB3 or VSV infection (Fig. 5f, g).

To figure out how CAP promotes type I IFNs production, we infected MEF with CVB3 and measured MDA5 and IRF3 protein expression. Indeed, MDA5 activation led to IRF3 phosphorylation and type I IFNs production [1]. As shown in Fig. 5h, MDA5 was properly expressed in the presence of CAP, while the absence of CAP was associated with a constant reduction of MDA5. Consequently, IRF3 phosphorylation was normal in infected $CAP^{+/+}$ MEF, but not in their $CAP^{-/-}$ counterparts (Fig 5h). These findings suggest that CAP is necessary for proper signalling transduction for type I IFNs production.

HeLa cells are suitable to study the function of CAP, since this cell line does not express endogenous CAP [47]. To figure out whether CAP reduces susceptibility to virus infections, we transfected HeLa cells with either a CAP-expressing vector or a mock vector as control. Transfected HeLa cells were then CVB3 infected and direct plaque assays were performed. As expected, CAP-transfected, but not mock-transfected HeLa cells, showed reduced viral proliferation (Fig. 5i, left). Similarly, MEF were infected with CVB3 for 24 h and cell lysates were used to test viral proliferation by plaque assay. Similar to transfected HeLa cells, CVB3-infected $CAP^{+/+}$ MEF showed lower viral proliferation compared to $CAP^{-/-}$ MEF (Fig. 5i, right). Since CAP is highly expressed in the heart [19, 46], we next addressed the role of CAP in mouse cardiac cells. Consequently, we measured the expression of type I and type II IFNs by real-time quantitative RT-PCR after infecting mouse neonatal cardiac fibroblasts (MNF) with CVB3. Both $CAP^{+/+}$ and $CAP^{-/-}$ cells expressed comparable high levels of IFN-β and IFN-γ, but IFN-α1 expression was significantly higher in $CAP^{+/+}$ MNF compared to $CAP^{-/-}$ MNF (Fig. 5j). These results suggest that increased IFN-α1 and IFN-β expression observed in $CAP^{+/+}$ hearts 4 days after CVB3 infection (Fig. 4a) reflects enhanced production of IFN-α1 by cardiac cells on one side, and IFN-β production by heart-infiltrating dendritic cells and macrophages on the other side.

To figure out if increased IFN-α1 expression in $CAP^{+/+}$ cardiac cells promotes antiviral protection, mouse neonatal cardiomyocytes (MNC) and MNF were infected in vitro with CVB3. Viral entry and viral proliferation were measured by reverse transcription of CVB3 genomic (+)RNA strand and (−)RNA strand sequences, respectively, which are then analysed by semi-quantitative RT-PCR [20]. CVB3 entry into cells is confirmed by the detection of the (+)RNA strand. The CVB3 (−)RNA strand, on the other

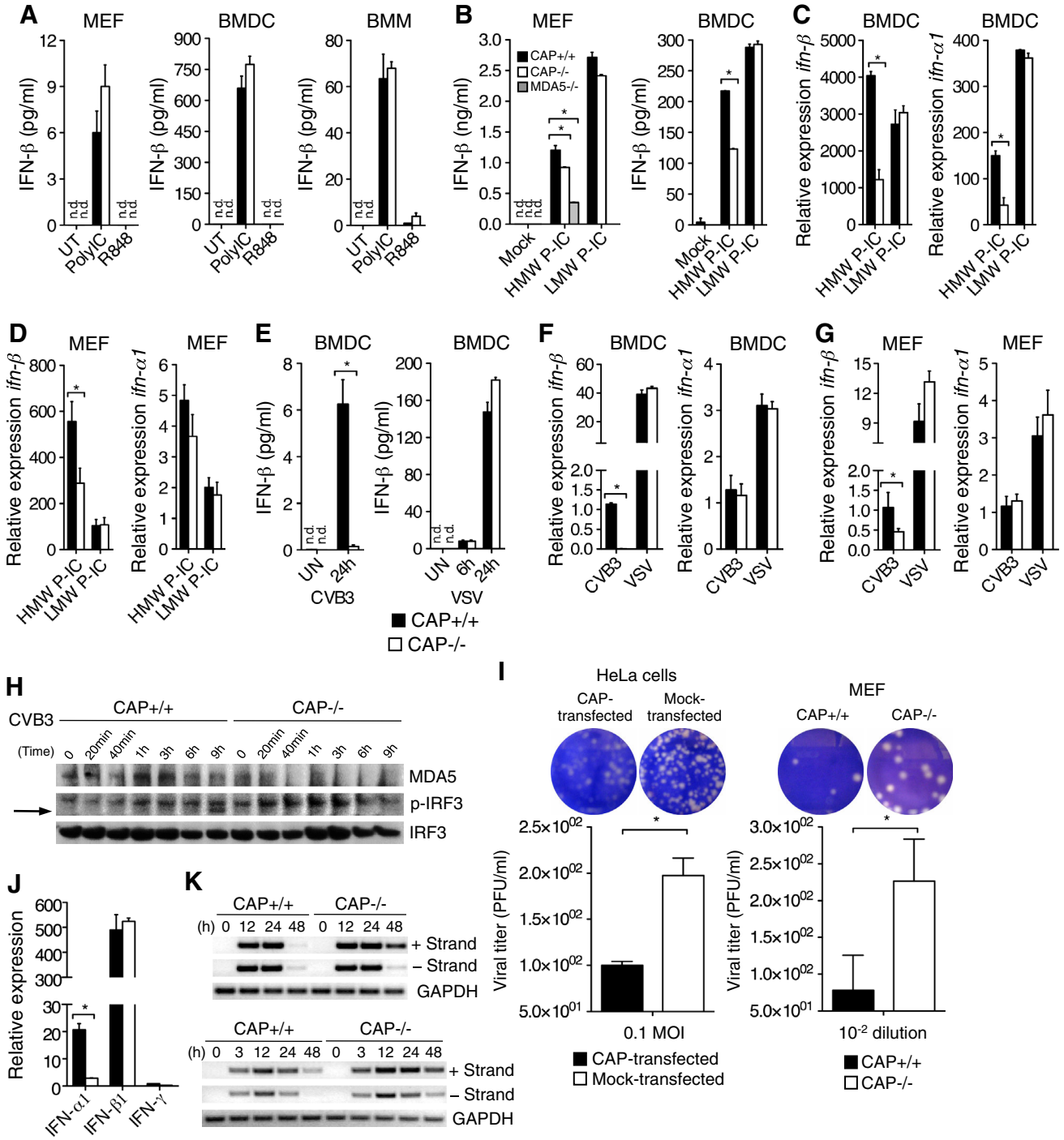
A
MEF
BMDC
BMM
IFN-β (pg/ml)
n.d.
UT
PolyIC
R848
B
MEF
BMDC
IFN-β (ng/ml)
IFN-β (pg/ml)
CAP+/+
CAP-/-
MDA5-/-
Mock
HMW P-IC
LMW P-IC
C
BMDC
BMDC
Relative expression ifn-β
Relative expression ifn-α1
D
MEF
MEF
Relative expression ifn-β
Relative expression ifn-α1
E
BMDC
BMDC
IFN-β (pg/ml)
UN
24h
6h
CVB3
VSV
CAP+/+
CAP-/-
F
BMDC
BMDC
Relative expression ifn-β
Relative expression ifn-α1
CVB3
VSV
G
MEF
MEF
Relative expression ifn-β
Relative expression ifn-α1
CVB3
VSV
H
CVB3
CAP+/+
CAP-/-
(Time)
0
20min
40min
1h
3h
6h
9h
MDA5
p-IRF3
IRF3
I
HeLa cells
CAP-transfected
Mock-transfected
MEF
CAP+/+
CAP-/-
Viral titer (PFU/ml)
0.1 MOI
10-2 dilution
CAP-transfected
Mock-transfected
CAP+/+
CAP-/-
J
Relative expression
IFN-α1
IFN-β1
IFN-γ
K
CAP+/+
CAP-/-
(h)
+ Strand
– Strand
GAPDH

◀**Fig. 5** CAP contributes to MDA5-dependent, but not TLR3/TLR7-dependent, production of type I IFNs. **a, b** IFN-β production in $CAP^{+/+}$ (*black bars*) and $CAP^{-/-}$ (*white bars*) MEF, BMDM, and BMM was measured in cell-free supernatants by ELISA after 24 h stimulation with 10 ng/ml PolyIC, 2.5 μg/ml R848, or left untreated (**a**) or 24 h after transfection with 1 ng/ml HMW-PolyIC, 1 ng/ml LMW-PolyIC, or mock (**b**). **c** Same BMDC (**c**) and MEF (**d**) as in (**b**), but harvested 6 h after transfection; IFN-β and IFN-α1 RNA levels were measured by qRT-PCR. **e** CVB3 at 1 MOI or VSV at 1 MOI were used for direct in vitro infection of BMDC. IFN-β was measured in cell-free supernatants by ELISA 24 h after infection. **f**, **g** BMDC (**f**) and MEF (**g**) were infected with 1 MOI CVB3 or 1 MOI VSV for 6 h; IFN-β and IFN-α1 RNA levels were measured by qRT-PCR. **h** MEF from $CAP^{+/+}$ and $CAP^{-/-}$ mice were infected with 1 MOI CVB3 for the indicated times. Immunoblot analysis of cell lysates performed with antibodies detecting MDA5, phosphorylated IRF-3, and total IRF-3. The *arrow points at the band* indicating phosphorylated IRF3. *UT* untreated. *UN* uninfected. *n.d.* not detected. **i** (*Left*) Plaque assay directly performed on HeLa cells transfected with CAP-encoding plasmid or mock-plasmid infected with CVB3 for 1 h and incubated in agar solution for 48 h. (*Right*) Cell lysates from $CAP^{+/+}$ and $CAP^{-/-}$ MEF infected for 48 h with CVB3 were used for plaque assay in HeLa cells. **j** Gene expression of IFN-α1, IFN-β, and IFN-γ in mouse neonatal cardiac fibroblasts 12 h after infection with 1 MOI CVB3, analysed by qRT-PCR. **k** Mouse neonatal cardiomyocytes (*top*) and mouse neonatal cardiac fibroblasts (*bottom*) infected with CVB3 at 1 MOI for the indicated times. Semi-quantitative RT-PCR performed with 1 μg RNA reverse transcribed with (+) strand CVB3 primers, (−) strand CVB3 primers, or random primers. GAPDH was reverse transcribed with random primers and used as internal control. Data are representative for three experiments performed in triplicates (mean, SD). $*P < 0.05$ (Student's *t* test)

hand, reflects the presence of viral replication intermediates, corresponding to viral proliferation [20]. As shown in Fig. 5k, both CVB3 (+)RNA and (−)RNA strands were reduced in $CAP^{+/+}$ MNC (Fig. 5k, top row) and MNF (Fig. 5k, bottom row) compared to their $CAP^{-/-}$ counterparts as early as 24 h after infection. Thus, CAP reduces CVB3 entry into cells as well as CVB3 replication. Mechanistically, the antiviral effect of CAP results from its role as a positive regulator of type I IFNs expression.

CAP supports MDA5 expression, while blocking MyD88

So far, we showed that CAP promotes type I IFN expression by enhanced phosphorylation of IRF3. However, the interaction between CAP and signalling molecules downstream of TLRs or RLRs receptors has not been investigated yet. To this end, we transfected HeLa cells with a CAP-encoding vector and infected them with CVB3. Immunoblotting of total cell lysates confirmed higher MDA5 expression before and after CVB3 infection in CAP-transfected cells compared to mock-transfected cells (Fig. 6a). IRF3, MyD88, and p65 as well as general protein poly- and monoubiquitination were similar (Fig. 6a). To analyse molecular interactions at different time points we immunoprecipitated FLAG-tagged CAP proteins. Looking at the most relevant proteins involved in CVB3-mediated type I IFNs production, we observed that MDA5 was the only molecule of the antiviral pathway, which interacted with CAP (Fig. 6b). Our observations were confirmed by co-immunoprecipitation of MDA5 with CAP-FLAG (Fig. 6c). Since relevant portions of the CAP protein, namely the SH3 sorbin domains, are needed to complex to the plasma membrane [5], we evaluated MDA5 expression in HeLa cells transfected with FLAG-tagged CAP-wt or a FLAG-tagged CAP plasmid lacking of its SH3 domains (CAP-ΔSH3). Immunoprecipitation of FLAG-tagged CAP showed that the SH3 domains are necessary for CAP to complex with MDA5, but total cell lysates analysis confirmed that MDA5 expression was not dependent on SH3 domains of CAP (Fig. 6d). Thus, CAP contributes to proper MDA5 expression.

In addition, we found that MyD88 was the only molecule of the NF-κB pathway, which complexed with CAP before CVB3 infection (Fig. 6b). Since MyD88 ubiquitination induces MyD88 degradation, which then downregulates the pro-inflammatory MyD88-dependent NF-κB pathway [24], we immunoprecipitated MyD88 and measured its ubiquitination. As hypothesized, MyD88 was ubiquitinated at a higher extent in CAP-transfected HeLa cells compared to mock-transfected HeLa cells after CVB3 infection (Fig. 6e).

Taken together, our data suggest that binding of CAP to MyD88 results in ubiquitination and degradation of this adaptor molecule and consequently inhibition of the MyD88-dependent pro-inflammatory pathway.

Discussion

In the present study, we provide for the first time evidence for a regulatory role of CAP in innate antiviral immunity. In fact, we found a dual role of CAP in promoting antiviral type I IFNs production, while reducing cytotoxic responses. Moreover, we recognized that CAP is part of the MDA5 complex that specifically recognizes (+)ssRNA viruses, such as the myocarditis-inducing CVB3, but not (−)ssRNA viruses.

To fight viral infections, the host activates several immune mechanisms to limit viral proliferation. Fast and prompt migration of lymphoid cells of myeloid origin, such as dendritic cells and macrophages, are critical for initial viral clearance. These cells produce IRF3-, IRF5-, and IRF7-dependent antiviral IFNs after identifying genomic particles of invading RNA viruses [15, 32, 42]. We have recently described the protective role of early heart-infiltrating monocytes/macrophages expressing the chemokine receptor CCR5 within 2 days after CVB3 infection [42]. In

parallel, host defence builds up $CD8^+$ T and NK cell-mediated responses to eliminate virus-infected cells. $CD8^+$ T and NK cells produce pore-forming perforin and granzymes that ultimately induce apoptosis of virus-infected cells [11]. Type I IFNs and cytotoxic proteins induce different antiviral responses. Indeed, type I IFNs, by binding to their receptors on the surface of dendritic cells and macrophages, promote the expression of IFN-stimulated genes (ISGs), such as Protein kinase R (PKR), 2′5′-oligoadenylate synthetase (OAS), Mx, viperin, and many others [28]. Co-ordinated activation of different ISGs can efficiently inhibit viral proliferation by blocking cell cycle of virus-infected cells, by preventing transport of incoming viral nucleocapsids into the cell nucleus, by interacting with viral capsids rendering virions non-infectious, or by inducing apoptosis of infected cells [28, 35]. Therefore, apoptosis induction in virus-infected cells is only one of several type I IFNs-mediated antiviral mechanisms protecting the host. Perforin and granzymes are necessary for proper viral clearance, but at the same time they induce the activation of apoptotic processes. The entry of perforin and granzymes into target cells is a pivotal step for initiating apoptosis leading to death of target cardiac cells [23]. Granzymes, and in particular granzyme B, induce cell apoptosis by activating Bid, dephosphorylating Bad, and promoting the release of Cytochrome c from the mitochondria, which ultimately results in caspase-dependent cell death [6, 39]. Perforin mediates cardiomyocyte injury in acute myocarditis caused by CVB3 [34]. It is also known that perforin induces higher mortality and increased myocarditis severity in CVB3-infected mice [10, 12]. CD8 T cells worsen myocarditis scores but reduce myocardial viral titers [13]. Our results therefore suggest that $CAP^{+/+}$ mice, which develop a strong type I IFN-dependent antiviral response and dampen cytotoxic cells, are subjected to less cardiac tissue injury than $CAP^{-/-}$ mice, which preferentially mount strong cytotoxic antiviral responses. Although $CAP^{-/-}$ hearts and spleens showed reduced viral proliferation at day 4 post CVB3 infection, we conclude that enhanced cytotoxicity renders $CAP^{-/-}$ mice more susceptible to CVB3-induced mortality during the first week after CVB3 inoculation.

Several studies describe perforin-producing lymphocytes in hearts of patients with viral myocarditis and in the hearts of CVB3-infected mice [33, 34, 45]. In addition, blockade of perforin with anti-perforin neutralizing antibodies limits cardiac cell injury in mice with viral myocarditis [12]. In our study, we observed increased expression of both perforin and granzyme B in hearts of $CAP^{-/-}$ CVB3-infected mice compared to $CAP^{+/+}$ CVB3-infected controls. Interestingly, perforin was higher in spleens of $CAP^{-/-}$ compared to $CAP^{+/+}$ CVB3-infected mice, while granzyme B showed comparable expression. At this time point, we cannot explain this observation, but a growing body of evidence points to granzyme B-independent, perforin-mediated cytotoxic mechanisms [14, 37]. Nevertheless, CAP reduces perforin-mediated cell apoptosis in the CVB3-infected heart.

In the present study, we found that CAP was necessary to induce IFN-β production upon MDA5 stimulation, but not upon TLR3, TLR7, and RIG-I activation. Indeed, MDA5, a cytosolic helicase with specificity toward positive double-strand RNA viruses [16], is one of the preferred targets of invading viruses. RNA viruses escape cellular antiviral responses by cleaving and degrading MDA5, thereby reducing type I IFNs production and increasing myocarditis susceptibility [4, 43]. Here, we found that CAP prevented MDA5 from CVB3-induced degradation. In addition, when CAP was expressed in HeLa cells, which are otherwise unable to produce CAP [47], MDA5 complexed with CAP after viral infection. We therefore conclude that CAP acts as a stabilizing molecule for MDA5, which in turn enhances antiviral responses against CVB3. Interestingly, in our pulling-down experiments, we observed that CAP complexed with MyD88, but not with other downstream proteins of the MyD88-IRAKs-TRAFs axis. Impaired or depleted MyD88 function results in general reduction of pro-inflammatory cytokine expression upon TLR activation except of TLR3 [1]. Nevertheless, future studies are needed to understand how exactly CAP-dependent modulation of MyD88 influences inflammatory cytokine expression.

Aside from antiviral mechanism, invading viruses can take advantage of the cellular structure of the host. Interaction with host transmembrane receptors in the heart, such as CAR and DAF, promotes conformational changes in the capsid of CVB3 that are essential for viral entry and release of viral RNA [7]. Intracellular signals triggered by both receptors include tyrosine kinase Lck, which is used by CVB3 to rearrange host cytoskeleton and thus increase viral entry [21]. Of note, Lck, apart from being target of CVB3, is well-known tyrosine kinase that promotes ZAP-70 recruitment for T cell receptor downstream signalling that activates T cells [38]. In the present study, we observed that CAP neither modified CAR nor Lck expression in the heart, but reduced Lck phosphorylation in splenocytes. By measuring the expression of CD69 and $CD44^{high}$, we confirmed that $CAP^{+/+}$ T cells were less activated and had lower memory/effector capacity than $CAP^{-/-}$ T cells. While reducing migration of cytotoxic $CD8^+$ T and NK cells, CAP also inhibited perforin and granzyme B production after viral infection in vivo and in vitro. Furthermore, transcription factors Eomes and T-bet, which are related to cytotoxicity [11, 40], were highly expressed in $CAP^{-/-}$ but not in $CAP^{+/+}$ spleen.

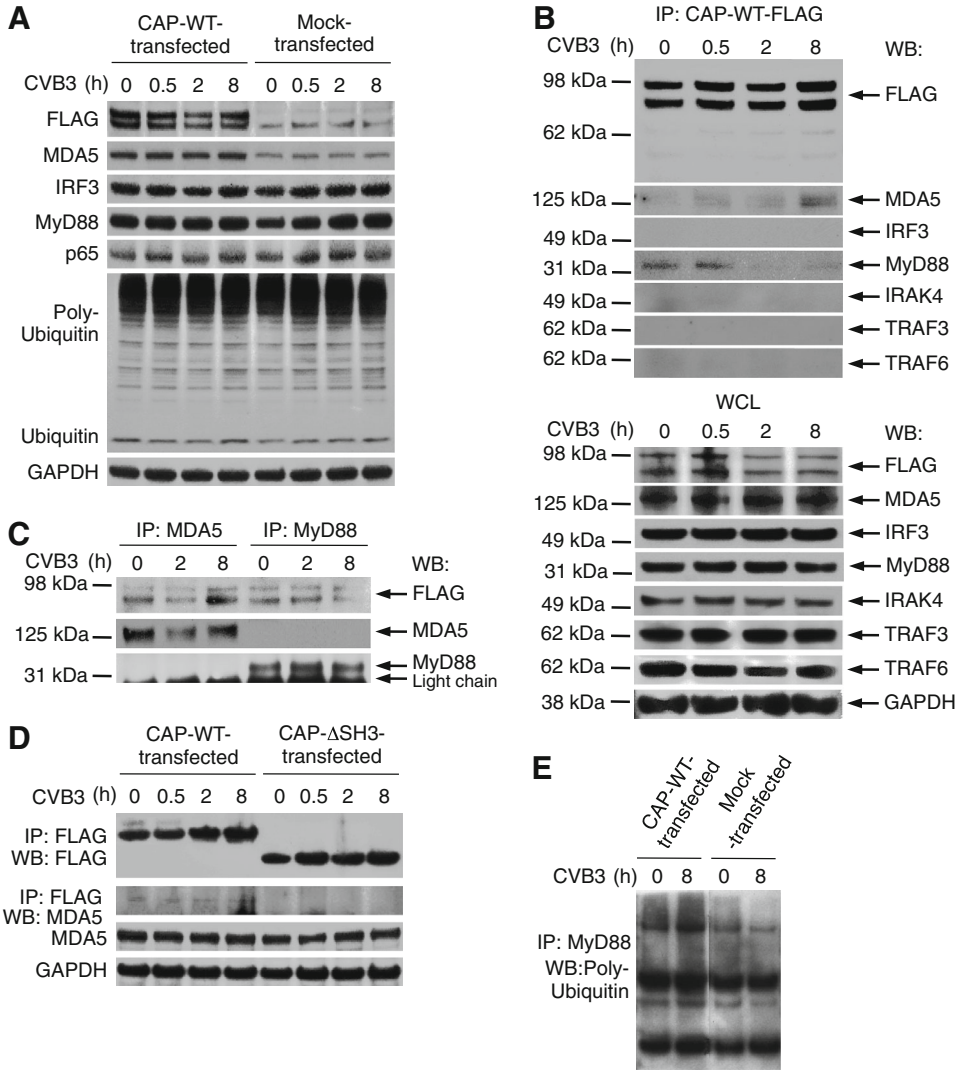

Fig. 6 CAP complexes with MDA5 and MyD88. **a** HeLa cells were transfected with CAP-wt-FLAG plasmid and then infected with 1 MOI CVB3 for the indicated times. Whole cell lysates (WCL) were immunoblotted with the indicated antibodies. **b** CAP-wt-FLAG-transfected HeLa cell lysates were immunoprecipitated with anti-FLAG antibodies and immunoblotted with the indicated antibodies (*top*). WCL were immunoblotted with the same antibodies (*below*). **c** HeLa cells were transfected with CAP-wt-FLAG plasmid and then infected with 1 MOI CVB3 for the indicated times. Cell lysates were immunoprecipitated with anti-MDA5 or anti-MyD88 antibodies and then immunoblotted with the indicated antibodies. **d** HeLa cells were transfected with CAP-wt-FLAG or CAP-ΔSH3-FLAG plasmid and then infected with 1 MOI CVB3 for the indicated times. FLAG immunoprecipitates of WCL were immunoblotted with the indicated antibodies. **e** CAP-wt-FLAG- or mock-transfected HeLa cells were immunoprecipitated with MyD88 and then immunoblotted with antibodies detecting polyubiquitin. Data are representative for two to three independent experiments

Taken together, we demonstrated for the first time a novel function of CAP as immune modulator in virus-induced cardiac inflammation. Our data show that CAP exerts a broad range of protective effects against (+)ssRNA virus infection, balancing immune responses towards a favourable outcome. CAP supports type I IFNs while reducing detrimental cytotoxic signals. Modulating CAP production might be a potential therapeutic strategy in acute viral myocarditis in the future, in particular to prevent end-stage heart failure.

Materials and methods

Mice, cells, viruses, and plasmids

Six- to eight-week-old CAP$^{-/-}$ male C57BL/6 mice (also known as Sorbs1$^{-/-}$ mice) were previously described [19]. All animal experiments were conducted in accordance with the Animal Care Committee of the University Health Network of the University of Toronto. Mouse embryonic fibroblasts (MEF) were cultivated using embryos at day

13.5 of gestation. Bone marrow-derived macrophages (BMM) and bone marrow-derived dendritic cells (BMDC) were cultivated as previously described [9, 41]. Mouse neonatal cardiomyocytes (MNC) were cultivated from the ventricles of 1-day-old newborns, digested with tripsin (0.8 mg/ml) and plated for 2 h at 37 °C to separate mouse neonatal cardiac fibroblasts (MNF) from MNC, and then cultivated in the presence of BrdU. The cardiovirulent CVB3 (Gauntt strain) has been described previously [20, 36], the vesicular stomatitis virus (VSV) was a gift of Dr. J. Bell. Viral titration in HeLa cells by standard plaque assay was performed as previously described [20, 36]. FLAG-tagged plasmids encoding CAP and CAP-ΔSH3 were a kind gift of Dr. Alan Saltiel [5, 47].

Histology

Cross sections of mouse hearts were hematoxylin and eosin stained as described [26], and evaluated for cellular infiltrates and necrosis as follows: 0, absence of infiltrating cells or necrosis; 1, limited focal areas of infiltrating cells or necrosis; 2, mild to moderate infiltrating cells or necrosis; 3, moderate infiltrating cells or necrosis; 4, extensive areas with infiltrating cells or necrosis involving the entire examined heart tissue.

Isolation of heart-infiltrating cells and flow cytometry analysis

Hearts were digested using Liberase TM Research Grade (Roche Diagnostics) at a working concentration of 0.08 Wuensch U/ml for 45 min at 37 °C. Heart-infiltrating cells were always triple-stained and first gated on live $CD45^{high}$ lymphocytes plotted on side-scatter/$CD45^{high}$ cells, acquired with a BD LSR II or a BD FACSCanto II (BD Biosciences), and analysed with FlowJo (Tree Star). Data were acquired until 200,000 events were collected from a live gate, as previously described [41].

Quantitative RT-PCR (qRT-PCR) and semi-quantitative RT-PCR

RNA was isolated with Trizol Reagent (Invitrogen) according to the manufacturer's protocol. Reverse transcription was performed with 1 μg RNA. The $2^{-\Delta\Delta Ct}$ method was used for qRT-PCR gene expression analysis. To reverse transcribe the CVB3 (+)RNA strand, we used the following primer: 5′-CACCGGATGGCCAATCCA-3′. To amplify its cDNA, we used the following primers for semi-quantitative RT-PCR:

(forward) 5′-CTCTCAATTGTCACCATAAGCAGCCA-3′;
(reverse) 5′-GCGAAGAGTCTATTGAGCTA-3′, as previously described [20].

Elisa

Commercially available VeriKine ELISA kit (PBL Interferon Source) was used to measure IFN-β.

Western blot analysis and immunoprecipitation

Tissue or cell lysates were separated using NuPAGE Novex Bis–Tris gel (Invitrogen), transferred on PVDF membrane (Roche Diagnostic), and then immunoblotted with specific antibodies. Bands were visualized with an ECL chemiluminescent substrate (Luminata Crescendo, Millipore). For immunoprecipitation, Dynabeads Protein G (Invitrogen) were used according to the manufacturer's instructions. FLAG-tagged proteins were immunoprecipitated using anti-DDK Tag (L5) Affinity Gel (Biolegend).

Reagents

High molecular weight (HMW) polyinosinic–polycytidylic acid (polyIC), low molecular weight (LMW) PolyIC, and the imidazoquinoline R848 were purchased from Invivogen. LPS and CpGs were purchased from Sigma.

Histopathology

Cross sections of paraffin-embedded hearts cut at 5 μm were stained with hematoxylin and eosin to evaluate inflammatory infiltrates reflecting myocarditis scores graded from 0 to 4 [25].

Echocardiography

Transthoracic 2D, M-mode, and Doppler echocardiographic studies were performed with an Acuson Sequoia C256 system equipped with a 15-MHz linear transducer (15L8) (Version 4.0, Acuson Corp) in mice anaesthetized with isoflurane/oxygen (1/100 %). M-mode tracings were recorded through these anterior and posterior LV walls at the papillary muscle level to measure LV end-diastolic dimension (LVEDD) and LV end-systolic dimension (LVESD). LV fractional shortening (FS) was calculated using the formula $FS = [(LVEDD - LVESD)/LVEDD] \times 100$.

Statistics

Survival rates were analysed by the Kaplan–Meier method, and differences between groups were tested with the log-rank test. Normally distributed data were compared using the unpaired two-tailed Student *t* test. Statistical analysis was conducted using the Prism 5 software (GraphPad Software). All data were expressed as mean ± SD. Differences were considered statistically significant for $P < 0.05$.

Acknowledgments Dr. Alan Valaperti got support from the Myocarditis Foundation and the Novartis Foundation. Dr. Urs Eriksson acknowledges support from the Swiss National Foundation. This work was supported in part by the Swiss National Foundation (SNF) and the Canadian Institutes of Health Research (CIHR).

Conflict of interest The authors declare that they have no conflict of interest.

References

1. Akira S, Uematsu S, Takeuchi O (2006) Pathogen recognition and innate immunity. Cell 124:783–801. doi:10.1016/j.cell.2006.02.015
2. Alexopoulou L, Holt AC, Medzhitov R, Flavell RA (2001) Recognition of double-stranded RNA and activation of NF-kappaB by Toll-like receptor 3. Nature 413:732–738. doi:10.1038/35099560
3. Anthony DA, Andrews DM, Watt SV, Trapani JA, Smyth MJ (2010) Functional dissection of the granzyme family: cell death and inflammation. Immunol Rev 235:73–92. doi:10.1111/j.0105-2896.2010.00907.x
4. Barral PM, Morrison JM, Drahos J, Gupta P, Sarkar D, Fisher PB, Racaniello VR (2007) MDA-5 is cleaved in poliovirus-infected cells. J Virol 81:3677–3684. doi:10.1128/JVI.01360-06
5. Baumann CA, Ribon V, Kanzaki M, Thurmond DC, Mora S, Shigematsu S, Bickel PE, Pessin JE, Saltiel AR (2000) CAP defines a second signalling pathway required for insulin-stimulated glucose transport. Nature 407:202–207. doi:10.1038/35025089
6. Carthy CM, Yanagawa B, Luo HL, Granville DJ, Yang DC, Cheung P, Cheung C, Esfandiarei M, Rudin CM, Thompson CB, Hunt DWC, McManus BM (2003) Bcl-2 and Bcl-xL overexpression inhibits cytochrome c release, activation of multiple caspases, and virus release following coxsackievirus B3 infection. Virology 313:147–157. doi:10.1016/S0042-6822(03)00242-3
7. Coyne CB, Bergelson JM (2006) Virus-induced Abl and Fyn kinase signals permit coxsackievirus entry through epithelial tight junctions. Cell 124:119–131. doi:10.1016/j.cell.2005.10.035
8. Datta SR, Ranger AM, Lin MZ, Sturgill JF, Ma YC, Cowan CW, Dikkes P, Korsmeyer SJ, Greenberg ME (2002) Survival factor-mediated BAD phosphorylation raises the mitochondrial threshold for apoptosis. Dev Cell 3:631–643. doi:10.1016/S1534-5807(02)00326-X
9. Eriksson U, Ricci R, Hunziker L, Kurrer MO, Oudit GY, Watts TH, Sonderegger I, Bachmaier K, Kopf M, Penninger JM (2003) Dendritic cell-induced autoimmune heart failure requires cooperation between adaptive and innate immunity. Nat Med 9:1484–1490. doi:10.1038/nm960
10. Gebhard JR, Perry CM, Harkins S, Lane T, Mena I, Asensio VC, Campbell IL, Whitton JL (1998) Coxsackievirus B3-induced myocarditis—Perforin exacerbates disease, but plays no detectable role in virus clearance. Am J Pathol 153:417–428. doi:10.1016/S0002-9440(10)65585-X
11. Glimcher LH, Townsend MJ, Sullivan BM, Lord GM (2004) Recent developments in the transcriptional regulation of cytolytic effector cells. Nat Rev Immunol 4:900–911. doi:10.1038/nri1490
12. Guo CY, Han B, Chang H, Jiang HL, Han XZ (2009) Anti-perforin neutralizing antibody reduces myocardial injury in viral myocarditis. Cardiol Young 19:601–607. doi:10.1017/S1047951110999182x
13. Henke A, Huber S, Stelzner A, Whitton JL (1995) The role of Cd8(+) T-lymphocytes in coxsackievirus B3-induced myocarditis. J Virol 69:6720–6728
14. Heusel JW, Wesselschmidt RL, Shresta S, Russell JH, Ley TJ (1994) Cytotoxic lymphocytes require Granzyme-B for the rapid induction of DNA fragmentation and apoptosis in allogeneic target-cells. Cell 76:977–987. doi:10.1016/0092-8674(94)90376-X
15. Honda K, Yanai H, Negishi H, Asagiri M, Sato M, Mizutani T, Shimada N, Ohba Y, Takaoka A, Yoshida N, Taniguchi T (2005) IRF-7 is the master regulator of type-I interferon-dependent immune responses. Nature 434:772–777. doi:10.1038/nature03464
16. Kato H, Takeuchi O, Sato S, Yoneyama M, Yamamoto M, Matsui K, Uematsu S, Jung A, Kawai T, Ishii KJ, Yamaguchi O, Otsu K, Tsujimura T, Koh CS, Reis e Sousa C, Matsuura Y, Fujita T, Akira S (2006) Differential roles of MDA5 and RIG-I helicases in the recognition of RNA viruses. Nature 441:101–105. doi:10.1038/nature04734
17. Kioka N, Ueda K, Amachi T (2002) Vinexin, CAP/ponsin, ArgBP2: a novel adaptor protein family regulating cytoskeletal organization and signal transduction. Cell Struct Funct 27:1–7. doi:10.1247/csf.27.1
18. Lebre AS, Jamot L, Takahashi J, Spassky N, Leprince C, Ravise N, Zander C, Fujigasaki H, Kussel-Andermann P, Duyckaerts C, Camonis JH, Brice A (2001) Ataxin-7 interacts with a Cbl-associated protein that it recruits into neuronal intranuclear inclusions. Hum Mol Genet 10:1201–1213. doi:10.1093/hmg/10.11.1201
19. Lesniewski LA, Hosch SE, Neels JG, de Luca C, Pashmforoush M, Lumeng CN, Chiang SH, Scadeng M, Saltiel AR, Olefsky JM (2007) Bone marrow-specific Cap gene deletion protects against high-fat diet-induced insulin resistance. Nat Med 13:455–462. doi:10.1038/nm1550
20. Liu P, Aitken K, Kong YY, Opavsky MA, Martino T, Dawood F, Wen WH, Kozieradzki I, Bachmaier K, Straus D, Mak TW, Penninger JM (2000) The tyrosine kinase p56lck is essential in coxsackievirus B3-mediated heart disease. Nat Med 6:429–434. doi:10.1038/74689
21. Maekawa Y, Ouzounian M, Opavsky MA, Liu PP (2007) Connecting the missing link between dilated cardiomyopathy and viral myocarditis: virus, cytoskeleton, and innate immunity. Circulation 115:5–8. doi:10.1161/CIRCULATIONAHA.106.670554
22. Mandai K, Nakanishi H, Satoh A, Takahashi K, Satoh K, Nishioka H, Mizoguchi A, Takai Y (1999) Ponsin/SH3P12: an l-afadin- and vinculin-binding protein localized at cell–cell and cell-matrix adherens junctions. J Cell Biol 144:1001–1017. doi:10.1083/jcb.144.5.1001
23. Mason JW (2003) Myocarditis and dilated cardiomyopathy: an inflammatory link. Cardiovasc Res 60:5–10. doi:10.1016/S0008-6363(03)00437-1
24. Naiki Y, Michelsen KS, Zhang W, Chen S, Doherty TM, Arditi M (2005) Transforming growth factor-beta differentially inhibits MyD88-dependent, but not TRAM- and TRIF-dependent, lipopolysaccharide-induced TLR4 signaling. J Biol Chem 280:5491–5495. doi:10.1074/jbc.C400503200
25. Opavsky MA, Martino T, Rabinovitch M, Penninger J, Richardson C, Petric M, Trinidad C, Butcher L, Chan J, Liu PP (2002) Enhanced ERK-1/2 activation in mice susceptible to coxsackievirus-induced myocarditis. J Clin Invest 109:1561–1569. doi:10.1172/JCI13971
26. Opavsky MA, Penninger J, Aitken K, Wen WH, Dawood F, Mak T, Liu P (1999) Susceptibility to myocarditis is dependent on the response of alphabeta T lymphocytes to coxsackieviral infection. Circ Res 85:551–558
27. Pichlmair A, Schulz O, Tan CP, Rehwinkel J, Kato H, Takeuchi O, Akira S, Way M, Schiavo G, Reis e Sousa C (2009) Activation of MDA5 requires higher-order RNA structures generated during

virus infection. J Virol 83:10761–10769. doi:10.1128/JVI.00770-09
28. Randall RE, Goodbourn S (2008) Interferons and viruses: an interplay between induction, signalling, antiviral responses and virus countermeasures. J Gen Virol 89:1–47. doi:10.1099/Vir.0.83391-0
29. Ribon V, Herrera R, Kay BK, Saltiel AR (1998) A role for CAP, a novel, multifunctional Src homology 3 domain-containing protein in formation of actin stress fibers and focal adhesions. J Biol Chem 273:4073–4080. doi:10.1074/jbc.273.7.4073
30. Ribon V, Printen JA, Hoffman NG, Kay BK, Saltiel AR (1998) A novel, multifuntional c-Cbl binding protein in insulin receptor signaling in 3T3-L1 adipocytes. Mol Cell Biol 18:872–879
31. Sagar S, Liu PP, Cooper LT Jr (2012) Myocarditis. Lancet 379:738–747. doi:10.1016/S0140-6736(11)60648-X
32. Sato M, Suemori H, Hata N, Asagiri M, Ogasawara K, Nakao K, Nakaya T, Katsuki M, Noguchi S, Tanaka N, Taniguchi T (2000) Distinct and essential roles of transcription factors IRF-3 and IRF-7 in response to viruses for IFN-alpha/beta gene induction. Immunity 13:539–548. doi:10.1016/S1074-7613(00)00053-4
33. Seko Y, Ishiyama S, Nishikawa T, Kasajima T, Hiroe M, Kagawa N, Osada K, Suzuki S, Yagita H, Okumura K, Yazaki Y (1995) Restricted usage of T-cell receptor V-Alpha-V-Beta genes in infiltrating cells in the hearts of patients with acute myocarditis and dilated cardiomyopathy. J Clin Invest 96:1035–1041. doi:10.1172/Jci118089
34. Seko Y, Shinkai Y, Kawasaki A, Yagita H, Okumura K, Yazaki Y (1993) Evidence of perforin-mediated cardiac myocyte injury in acute murine myocarditis caused by coxsackie virus-B3. J Pathol 170:53–58. doi:10.1002/Path.1711700109
35. Sen GC (2001) Viruses and interferons. Annu Rev Microbiol 55:255–281. doi:10.1146/Annurev.Micro.55.1.255
36. Shi Y, Fukuoka M, Li G, Liu Y, Chen M, Konviser M, Chen X, Opavsky MA, Liu PP (2010) Regulatory T cells protect mice against coxsackievirus-induced myocarditis through the transforming growth factor beta-coxsackie-adenovirus receptor pathway. Circulation 121:2624–2634. doi:10.1161/CIRCULATIONAHA.109.893248
37. Shresta S, Russell JH, Ley TJ (1997) Mechanisms responsible for granzyme B-independent cytotoxicity. Blood 89:4085–4091
38. Smith-Garvin JE, Koretzky GA, Jordan MS (2009) T cell activation. Annu Rev Immunol 27:591–619. doi:10.1146/annurev.immunol.021908.132706
39. Taylor RC, Cullen SP, Martin SJ (2008) Apoptosis: controlled demolition at the cellular level. Nat Rev Mol Cell Biol 9:231–241. doi:10.1038/Nrm2312
40. Townsend MJ, Weinmann AS, Matsuda JL, Salomon R, Farnham PJ, Biron CA, Gapin L, Glimcher LH (2004) T-bet regulates the terminal maturation and homeostasis of NK and Valpha14i NKT cells. Immunity 20:477–494. doi:10.1016/S1074-7613(04)00076-7
41. Valaperti A, Marty RR, Kania G, Germano D, Mauermann N, Dirnhofer S, Leimenstoll B, Blyszczuk P, Dong C, Mueller C, Hunziker L, Eriksson U (2008) CD11b+ monocytes abrogate Th17 CD4+ T cell-mediated experimental autoimmune myocarditis. J Immunol 180:2686–2695
42. Valaperti A, Nishii M, Liu Y, Naito K, Chan M, Zhang L, Skurk C, Schultheiss HP, Wells GA, Eriksson U, Liu PP (2013) Innate immune interleukin-1 receptor-associated kinase 4 exacerbates viral myocarditis by reducing CCR5(+) CD11b(+) monocyte migration and impairing interferon production. Circulation 128:1542–1554. doi:10.1161/CIRCULATIONAHA.113.002275
43. Wang JP, Cerny A, Asher DR, Kurt-Jones EA, Bronson RT, Finberg RW (2010) MDA5 and MAVS mediate type I interferon responses to coxsackie B virus. J Virol 84:254–260. doi:10.1128/JVI.00631-09
44. Yajima T, Knowlton KU (2009) Viral myocarditis: from the perspective of the virus. Circulation 119:2615–2624. doi:10.1161/CIRCULATIONAHA.108.766022
45. Young LHY, Joag SV, Zheng LM, Lee CP, Lee YS, Young JDE (1990) Perforin-mediated myocardial damage in acute myocarditis. Lancet 336:1019–1021. doi:10.1016/0140-6736(90)92486-2
46. Zhang M, Kimura A, Saltiel AR (2003) Cloning and characterization of Cbl-associated protein splicing isoforms. Mol Med 9:18–25
47. Zhang M, Liu J, Cheng A, Deyoung SM, Chen X, Dold LH, Saltiel AR (2006) CAP interacts with cytoskeletal proteins and regulates adhesion-mediated ERK activation and motility. EMBO J 25:5284–5293. doi:10.1038/sj.emboj.7601406
48. Ziemba SE, Menard SL, McCabe MJ Jr, Rosenspire AJ (2009) T-cell receptor signaling is mediated by transient Lck activity, which is inhibited by inorganic mercury. FASEB J 23:1663–1671. doi:10.1096/fj.08-117283